Stanford Exploration Project, Report 100, April 20, 1999, pages 125–135

Extending common-azimuth migration

Louis Vaillant and Biondo Biondi[1]

keywords: *common-azimuth, prestack depth migration, stationary phase*

ABSTRACT

We present a review of common-azimuth prestack depth migration theory and propose a new extension to the original method. In common-azimuth migration theory, source and receiver raypaths are constrained to lie on the same plane at each depth level. By using data with a broader range of cross-line offsets, we increase the number of raypaths examined and consider more information. Consequently, our extended common-azimuth migration is theoretically better able to model lateral velocity variations due to real 3-D structures and is more compatible with the standard marine acquisition geometry, in which cross-line offsets are concentrated in a narrow band. We first discuss the theory of the process, and then introduce computational issues leading to future implementation.

INTRODUCTION

Common-azimuth migration was first introduced by Biondi and Palacharla (1994). It is a 3-D depth imaging method based on a recursive downward continuation of prestack data, and allows a robust and accurate depth migration since it is derived directly from the full wave equation. As opposed to Kirchhoff methods, common-azimuth migration is not derived from asymptotic approximations, and thus it represents a potentially robust alternative to Kirchhoff methods for 3-D prestack migration.

The implementation of wave-equation methods presents several difficulties. Whereas Kirchhoff methods handle irregular geometries relatively easily, the downward-continuation process needs data with a regular geometry in order to correctly propagate the wavefield. Additionally, full volume 3-D wave equation migration still has a high computational cost. The challenge for such a recursive algorithm is to extrapolate the wavefield in a 5-D space: time, in-line and cross-line midpoint coordinates, and in-line and cross-line offsets, (t, m_x, m_y, h_x, h_y). This computation is still beyond the reach of current computer technology. We can address this problem by only downward continuing common-azimuth data for which $h_y = 0$. In this way, the data space is reduced to 4-D. Common-azimuth data are obtained through azimuth moveout (AMO), which rotates and modifies the offset of 3-D prestack data (Biondi et al., 1998). AMO is used as a preprocessing step to regularize the

[1]**email:** louis@sep.stanford.edu, biondo@sep.stanford.edu

3-D data acquisition, and organize it in sets of constant cross-line offset. The first section discusses the original method, and the second one presents its new extension.

COMMON-AZIMUTH PHASE-SHIFT MIGRATION

One way to reduce the computational cost of 3-D prestack depth migration is to use common-azimuth data, which is only a 4-D dataset. Common-azimuth migration is then derived as the solution of the one-way wave equation through a recursive downward-continuation operator. In the frequency-wavenumber domain, this operator can be expressed as a simple phase-shift applied to the wavefield. We use the notation indicated below. The vertical wavenumber k_z is given by a 3-D dispersion relation called the Double Square Root (DSR) equation (Claerbout, 1984):

$$\begin{aligned} DSR(\omega, \mathbf{k}_m, \mathbf{k}_h, z) = \quad & \sqrt{\frac{\omega^2}{v(\mathbf{r},z)^2} - \frac{1}{4}\left[(k_{mx}+k_{hx})^2 + (k_{my}+k_{hy})^2\right]} \\ & + \sqrt{\frac{\omega^2}{v(\mathbf{s},z)^2} - \frac{1}{4}\left[(k_{mx}-k_{hx})^2 + (k_{my}-k_{hy})^2\right]} \end{aligned} \tag{1}$$

where $\mathbf{k}_m$ is the midpoint wavenumber ($\mathbf{k}_m = k_{mx}\mathbf{x}_m + k_{my}\mathbf{y}_m$), $\mathbf{k}_h$ the offset wavenumber ($\mathbf{k}_h = k_{hx}\mathbf{x}_h + k_{hy}\mathbf{y}_h$) and k_z the vertical wavenumber ($k_z = DSR(\omega, \mathbf{k}_m, \mathbf{k}_h, z)$), with $\mathbf{x}_m$, $\mathbf{y}_m$, $\mathbf{x}_h$ and $\mathbf{y}_h$ unit vectors of the four midpoint and offset axes. The propagation velocities $v(\mathbf{r}, z)$ and $v(\mathbf{s}, z)$ correspond respectively to the receiver and source locations.

The first square root in equation (1) downward-continues the receiver wavefield, whereas the second one downward-continues the source wavefield. In the algorithm developed by Biondi and Palacharla (1996), the data at the new depth level D_{z+dz} are obtained from common-azimuth data D_z by the following integration:

$$\begin{aligned} D_{z+dz}(\omega, \mathbf{k}_m, k_{hx}, h_y = 0) &= \int_{-\infty}^{+\infty} D_z(\omega, \mathbf{k}_m, k_{hx}, h_y = 0) e^{-ik_z dz} dk_{hy} \\ &= D_z(\omega, \mathbf{k}_m, k_{hx}, h_y = 0) \int_{-\infty}^{+\infty} e^{-ik_z dz} dk_{hy} \\ &= D_z(\omega, \mathbf{k}_m, k_{hx}, h_y = 0) \times \text{Down}(\omega, \mathbf{k}_m, k_{hx}, z) \end{aligned} \tag{2}$$

In practice, we use the stationary-phase approximation to compute this integral (see Appendix A). Popovici (1995) finds a very similar expression for the kernel of migration to zero-offset (MZO) in 2-D and asserts that the stationary-phase approximation avoids the very high computational cost of a numerical evaluation of the integral.

In our case, the stationary phase approximation of the common-azimuth downward-continuation operator for data where $h_y = 0$ can be written as

$$\text{Down}(\omega, \mathbf{k}_m, k_{hx}, z) = \sqrt{\frac{2\pi}{\phi''\left(\hat{k}^0_{hy}\right)}}\, e^{-i\phi\left(\hat{k}^0_{hy}\right) + i\frac{\pi}{4}} \tag{3}$$

with the phase $\phi = DSR(\omega, \mathbf{k}_m, \mathbf{k}_h, z)dz$.

For data evaluated only at the origin of the cross-line offset axis ($h_y = 0$), Biondi and Palacharla (1996) derived an analytical expression for the stationary point:

$$\hat{k}_{hy}^0(z) = k_{my} \frac{\sqrt{\frac{1}{v(\mathbf{r},z)^2} - \frac{1}{4\omega^2}(k_{mx}+k_{hx})^2} - \sqrt{\frac{1}{v(\mathbf{s},z)^2} - \frac{1}{4\omega^2}(k_{mx}-k_{hx})^2}}{\sqrt{\frac{1}{v(\mathbf{r},z)^2} - \frac{1}{4\omega^2}(k_{mx}+k_{hx})^2} + \sqrt{\frac{1}{v(\mathbf{s},z)^2} - \frac{1}{4\omega^2}(k_{mx}-k_{hx})^2}} \tag{4}$$

We have implemented the kernel of downward-continuation and phase-shift migration with the preceding theory. Simulations performed with the standard common-azimuth migration code have already proven its efficiency in imaging complex media (Biondi, 1999). As shown in Figures 1 and 2, the common-azimuth technique provides accurate subsalt images. Still, on the left side of Figure 1(b), imaging the major fault has obviously met with some difficulties, which can be attributed to rapid lateral variations of the velocity model. As seen in Figures 2(a) and 2(b), the same fault, now on the right side, is also dipping in the cross-line direction. Extending the common-azimuth technique may help improve the imaging of these lateral velocity variations.

EXTENDING CROSS-LINE OFFSET RANGE

Marine data usually contain in-line offsets up to 3-5km, and only show a narrow range of offsets in the cross-line direction. For standard common-azimuth migration, AMO is used to rotate the data to zero cross-line offset. What we do now is use AMO to regularize the acquisition but organize data along several near-zero cross-line offsets. Strictly speaking, the data are not "common-azimuth", but "quasi-common-azimuth" or "narrow-azimuth" since we have only a narrow range of cross-line offsets.

These narrow-azimuth data $D_z(\omega, \mathbf{k}_m, k_{hx}, h_y)$ are downward-continued as before, with an important difference in the phase of the integrand:

$$\begin{aligned} D_{z+dz}(\omega, \mathbf{k}_m, k_{hx}, h_y) &= \int_{-\infty}^{+\infty} D_z(\omega, \mathbf{k}_m, k_{hx}, h_y) e^{-ik_z dz} e^{-ik_{hy} h_y} dk_{hy} \\ &= D_z(\omega, \mathbf{k}_m, k_{hx}, h_y) \int_{-\infty}^{+\infty} e^{-ik_z dz} e^{-ik_{hy} h_y} dk_{hy} \\ &= D_z(\omega, \mathbf{k}_m, k_{hx}, h_y) \times \text{Down}(\omega, \mathbf{k}_m, k_{hx}, z) \end{aligned} \tag{5}$$

with

$$\begin{aligned} \text{Down}(\omega, \mathbf{k}_m, k_{hx}, z) &= \sqrt{\frac{2\pi}{\phi''\left(\hat{k}_{hy}\right)}} e^{-i\phi\left(\hat{k}_{hy}\right) + i\frac{\pi}{4}} \\ \phi &= DSR(\omega, \mathbf{k}_m, \mathbf{k}_h, z)dz + k_{hy} h_y \end{aligned} \tag{6}$$

In 2-D, for the case of a phase-shift migration in which the equations are similar to ours, Alkhalifah (1997) found that solving for the minimum of the phase ϕ involves a sixth-order

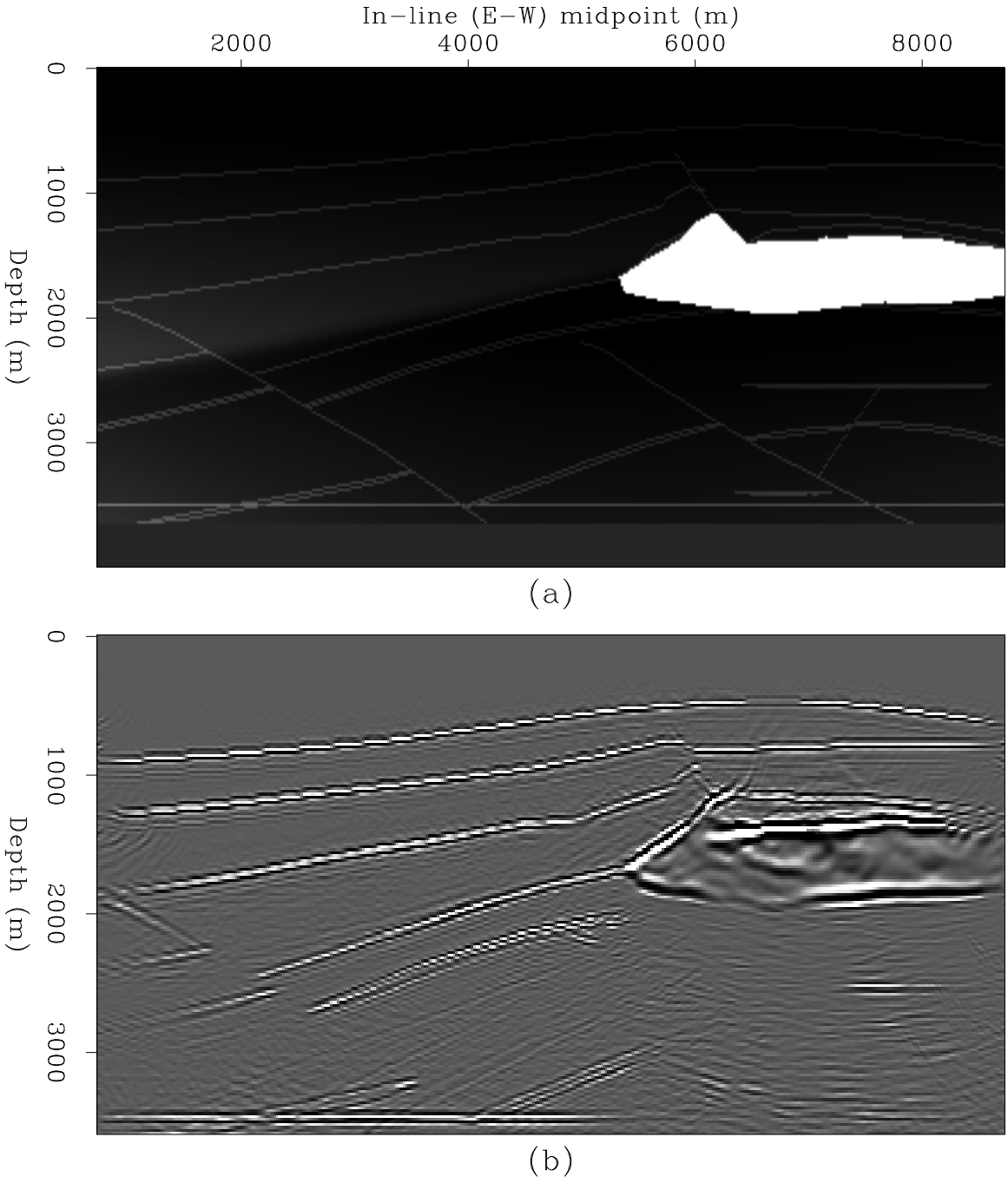

Figure 1: Common-azimuth prestack depth migration of data from the SEG-EAGE salt model. In-line section at CMPy=10400 (m). The top plot (a) represents the exact velocity model and the bottom plot (b) represents the migration result. louis1-SEG-EAGE-in [CR]

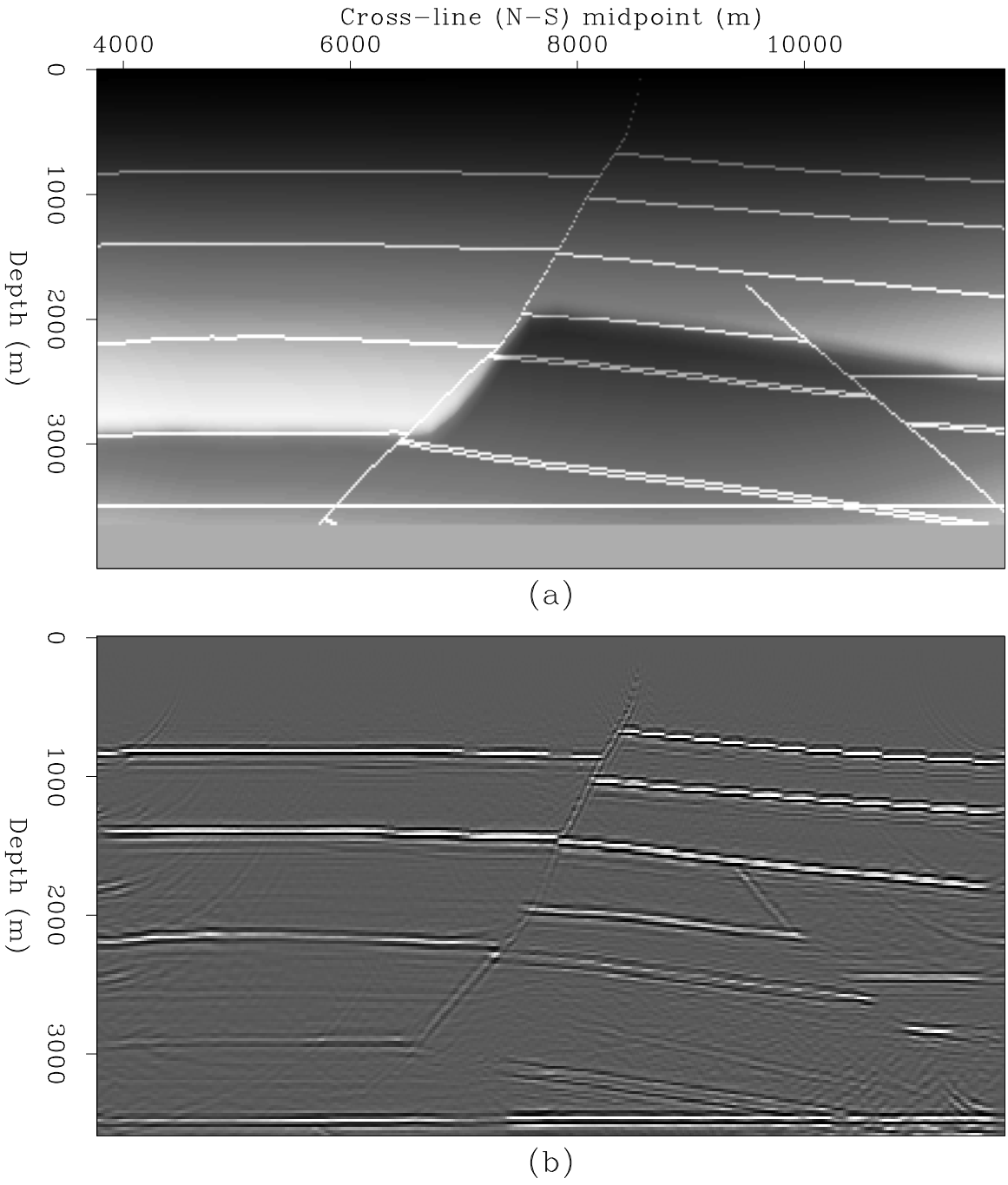

Figure 2: Common-azimuth prestack depth migration of data from the SEG-EAGE salt model. Cross-line section at CMPx=2100 (m). The top plot (a) represents the exact velocity model and the bottom plot (b) represents the migration result. louis1-SEG-EAGE-cross [CR]

polynomial, making it difficult to find an analytical expression of the stationary path. Thus, since we are unable to use such an analytical expression for non-zero h_y, we instead use only a range of values of $\hat{k}_{hy}$ centered around the stationary path $\hat{k}^0_{hy}$, which is given by equation (4), at zero cross-line offset. At each $\hat{k}_{hy}$, a different phase shift is applied: the data $D_z(\omega, \mathbf{k}_m, k_{hx}, h_y)$ are transformed by modulation and FFT along the cross-line offset axis into $\widetilde{D}_z(\omega, \mathbf{k}_m, k_{hx}, k_{hy})$, in which the range of the coordinate k_{hy} is centered around $\hat{k}^0_{hy}$. Then we apply the phase shift, $\phi(\hat{k}_{hy})$, for each value of the set $\{\hat{k}_{hy} = \hat{k}^0_{hy} \pm i_{k_{hy}} dk_{hy}\}$.

The reformulation of the problem has some interesting geometrical consequences. In the case of standard common-azimuth migration, the stationary path of phase ϕ derived in equation (4) is equivalent to the following relationship between the ray parameters (Biondi, 1998):

$$\frac{p_{sy}}{p_{sz}} = \frac{p_{ry}}{p_{rz}} \tag{7}$$

The subscript, s, refers to the source ray, and, r, to the receiver ray:

$$p_{sx} = \frac{k_{mx} - k_{hx}}{2\omega} \qquad p_{rx} = \frac{k_{mx} + k_{hx}}{2\omega} \qquad p_{sy} = \frac{k_{my} - k_{hy}}{2\omega} \qquad p_{ry} = \frac{k_{my} + k_{hy}}{2\omega}$$

The ray parameters are linked by the relationship:

$$p_{sx}^2 + p_{sy}^2 + p_{sy}^2 = \frac{1}{v(\mathbf{s}, z)^2} \qquad p_{rx}^2 + p_{ry}^2 + p_{ry}^2 = \frac{1}{v(\mathbf{r}, z)^2}$$

Equation (7) constrains the source ray and the receiver ray to lie on the same plane between depths z and $z + dz$, so that the sources and receivers at the new depth are aligned along the same azimuth as at the preceding depth (Figure 3). Assuming this constraint, common-azimuth migration is not strictly correct even in the simple case of a $v(z)$ medium (Figure 4). Since the projections of the source and receiver rays on a cross-line plane do not coincide unless the angles α and β are equal, azimuth is not conserved at each depth step of downward continuation. As a general consequence, local variations in velocity, which cause ray bending phenomena, introduce an error in the computation of the common-azimuth downward continuation. Biondi and Palacharla (1996) put forward that this error is small, but by using several discrete values of k_{hy} in a neighborhood of $\hat{k}^0_{hy}$, we hope to improve the result.

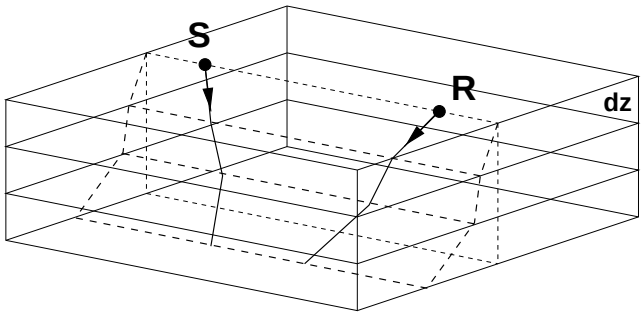

Figure 3: Schematic showing the ray geometry for common-azimuth downward continuation. louis1-ray-comaz [NR]

The narrow-azimuth approach may improve the imaging process by better taking velocity variations into account (Figure 5). Lateral velocity variations, for example, can make rays

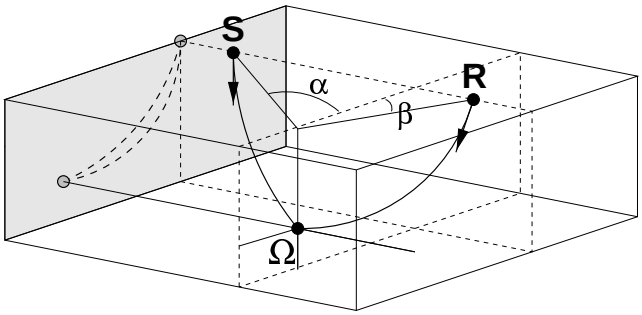

Figure 4: Schematic showing the ray geometry for common-azimuth downward continuation in a simple $v(z)$ velocity model. The projections of both rays on a cross-line plane do not coincide due to non-conservation of azimuth at each depth level. louis1-ray-vofz [NR]

bend in the cross-line direction, and even make rays start in different planes before they converge to a deeper reflection point. The bending due to real 3-D structures is implicitly eliminated when strictly zero-azimuth data are downward continued, whereas we would like to keep it for an extension of common-azimuth migration.

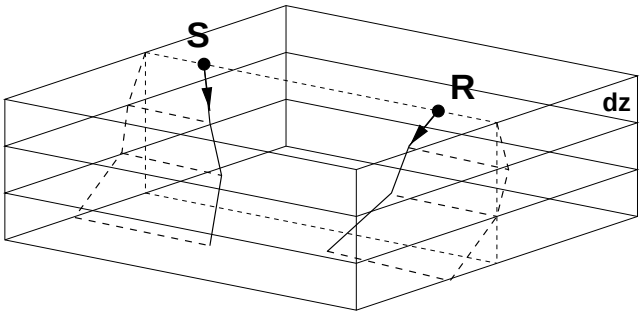

Figure 5: Schematic showing the ray geometry for narrow-azimuth downward continuation. A larger range of cross-line offsets will allow the modeling of lateral variations in the velocity model by taking into consideration rays not lying in the same slanted plane. louis1-ray-extended [NR]

Our approximation, using a neighborhood of $\hat{k}^0_{hy}$, is valid if the stationary path, $\hat{k}_{hy}$, varies slowly with h_y around the analytical solution, $\hat{k}^0_{hy}$. To estimate these variations, we can use the Implicit Function theorem: the equation $\frac{\partial \phi}{\partial k_{hy}} = 0$, which gives the stationary path $\hat{k}_{hy}$, also defines a relation of the general form $F(k_{hy}, h_y) = 0$. Thus, in a neighborhood of the solution $\hat{k}_{hy}$, we use a function $k_{hy}(h_y)$, whose variations are determined by the inverse of the phase second derivative:

$$\left(\frac{dk_{hy}}{dh_y}\right)_{\hat{k}_{hy}} = -\frac{\frac{\partial^2 \phi}{\partial h_y \partial k_{hy}}}{\frac{\partial^2 \phi}{\partial k^2_{hy}}} = -\left(\frac{\partial^2 \phi}{\partial k^2_{hy}}\right)^{-1} \tag{8}$$

We now need to examine the variations of the phase with k_{hy}. We introduced the ray parameter notation in equation (4). Therefore the phase has the expression shown in equation (9). We can calculate its first and second partial derivatives with respect to k_{hy} (see Appendix B):

$$\phi = \omega dz \left\{ \sqrt{\frac{1}{v(\mathbf{r}, z)^2} - \left(p^2_{rx} + p^2_{ry}\right)} + \sqrt{\frac{1}{v(\mathbf{s}, z)^2} - \left(p^2_{sx} + p^2_{sy}\right)} \right\} + k_{hy} h_y \tag{9}$$

$$\frac{\partial \phi}{\partial k_{hy}} = dz \left\{ \frac{-p_{ry}}{2\sqrt{\frac{1}{v(\mathbf{r},z)^2} - \left(p_{rx}^2 + p_{ry}^2\right)}} + \frac{p_{sy}}{2\sqrt{\frac{1}{v(\mathbf{s},z)^2} - \left(p_{sx}^2 + p_{sy}^2\right)}} \right\} + h_y \qquad (10)$$

$$\frac{\partial^2 \phi}{\partial k_{hy}^2} = -\frac{dz}{4\omega} \left\{ \frac{\left(\frac{1}{v(\mathbf{r},z)^2} - p_{rx}^2\right)}{\left(\frac{1}{v(\mathbf{r},z)^2} - \left(p_{rx}^2 + p_{ry}^2\right)\right)^{\frac{3}{2}}} + \frac{\left(\frac{1}{v(\mathbf{s},z)^2} - p_{sx}^2\right)}{\left(\frac{1}{v(\mathbf{s},z)^2} - \left(p_{sx}^2 + p_{sy}^2\right)\right)^{\frac{3}{2}}} \right\} \leq 0 \qquad (11)$$

According to equation (6), the computation process will blow up if the second derivative becomes close to zero. The failure happens for (and only for) $p_{rx} = \frac{1}{v}$, corresponding to the quasi-horizontal propagation of evanescent waves. We also see that the second derivative is independent from the value of the cross-line offset, h_y. This means that the variations of k_{hy} with h_y, given by equation (8), will be the same around each stationary point.

Ideally, we would like to have small variations of the stationary path with h_y, in order to use correctly values of k_{hy} around the known solution $\hat{k}_{hy}^0$ for the stationary points $\hat{k}_{hy}$, which we cannot determine analytically. Small variations mean a high value of the phase second derivative in equation (11). When the derivative is close to zero, problems in the computation may arise, but this will never happen for waves propagating downward. The "limiting" case is horizontal propagation. It means that narrow-azimuth migration may not completely overcome the steep-dip limitations of common-azimuth migration.

CONCLUSION AND FUTURE WORK

We have presented a review of common-azimuth prestack depth migration theory and proposed an extension to improve the imaging where there are strong lateral variations of the velocity model. Since the extended code is still "work in progress," we are not, as yet, able to present concrete results. We intend to test the program in the case of a simple $V(z)$ medium and with more complex synthetics, before applying both common-azimuth and narrow-azimuth on a real dataset adequately preprocessed with AMO.

ACKNOWLEDGEMENTS

We would like to thank Elf Aquitaine for providing the data and supporting this study. We thank in particular Henri Calandra for his help and fruitful discussions.

REFERENCES

Alkhalifah, T., 1997, Prestack time migration for anisotropic media: SEP–**94**, 263–298.

Biondi, B., and Palacharla, G., 1994, 3-D prestack migration of common-azimuth data: SEP–**80**, 109–124.

Biondi, B., and Palacharla, G., 1996, 3-D prestack migration of common-azimuth data: Geophysics, **61**, no. 6, 1822–1832.

Biondi, B., Fomel, S., and Chemingui, N., 1998, Azimuth moveout for 3-D prestack imaging: Geophysics, **63**, no. 2, 574–588.

Biondi, B. 3-D Seismic Imaging:. http://sepwww.stanford.edu/sep/biondo/Lectures, 1998.

Biondi, B., 1999, Subsalt imaging by common-azimuth migration: SEP–**100**, 113–124.

Bleistein, N. Mathematical methods for wave phenomena:. Academic Press, 1984.

Claerbout, J. F., 1984, Imaging the Earth's Interior: SEP–**40**.

Popovici, A. M., 1995, Migration to zero offset in variable velocity media: Ph.D. thesis, Stanford University.

APPENDIX A

The stationary phase theorem announces the following result (Bleistein, 1984):

Integrals of the form

$$I(k) = \int_{-\infty}^{+\infty} e^{ik\phi(t)} f(t) dt \tag{A-1}$$

can be approximated asymptotically when $k \to \infty$ by:

$$I(k) \approx \sqrt{\frac{2\pi}{k|\phi''(t_0)|}} f(t_0) e^{ik\phi(t_0)+sgn(\phi''(t_0))\frac{i\pi}{4}} \tag{A-2}$$

where t_0 is the stationary point at which the phase derivative $\phi'(t) = 0$, $f(t)$ is a complex function, and the phase $\phi(t)$ is real.

The method is based on a high-frequency approximation, the general idea being that the integral has most of its area near the stationary point t_0. The approximate value of the integral in the neighborhood of the stationary point is then obtained analytically by expanding $\phi(t)$ and $f(t)$ in a Taylor series around t_0.

APPENDIX B

We develop here the calculation of the second derivative of the phase from its expression in narrow-azimuth migration:

$$\phi = DSR(\omega, \mathbf{k}_m, \mathbf{k}_h, z)dz + k_{hy} h_y$$

$$= \omega dz \left\{ \sqrt{\frac{1}{v(\mathbf{r},z)^2} - \left(p_{rx}^2 + p_{ry}^2\right)} + \sqrt{\frac{1}{v(\mathbf{s},z)^2} - \left(p_{sx}^2 + p_{sy}^2\right)} \right\} + k_{hy} h_y$$

$$\begin{aligned}
\frac{\partial^2 \phi}{\partial k_{hy}^2} &= \frac{dz}{4\omega} \frac{-\sqrt{\frac{1}{v(\mathbf{r},z)^2} - \left(p_{rx}^2 + p_{ry}^2\right)} - p_{ry} \frac{p_{ry}}{\sqrt{\frac{1}{v(\mathbf{r},z)^2} - \left(p_{rx}^2 + p_{ry}^2\right)}}}{\frac{1}{v(\mathbf{r},z)^2} - \left(p_{rx}^2 + p_{ry}^2\right)} \\
&\quad + \frac{dz}{4\omega} \frac{-\sqrt{\frac{1}{v(\mathbf{s},z)^2} - \left(p_{sx}^2 + p_{sy}^2\right)} - p_{sy} \frac{p_{sy}}{\sqrt{\frac{1}{v(\mathbf{s},z)^2} - \left(p_{sx}^2 + p_{sy}^2\right)}}}{\frac{1}{v(\mathbf{s},z)^2} - \left(p_{sx}^2 + p_{sy}^2\right)} \\
&= \frac{dz}{4\omega} \left\{ \frac{-\frac{1}{v(\mathbf{r},z)^2} + \left(p_{rx}^2 + p_{ry}^2\right) - p_{ry}^2}{\left(\frac{1}{v(\mathbf{r},z)^2} - \left(p_{rx}^2 + p_{ry}^2\right)\right)^{\frac{3}{2}}} + \frac{-\frac{1}{v(\mathbf{s},z)^2} + \left(p_{sx}^2 + p_{sy}^2\right) - p_{sy}^2}{\left(\frac{1}{v(\mathbf{s},z)^2} - \left(p_{sx}^2 + p_{sy}^2\right)\right)^{\frac{3}{2}}} \right\} \\
\frac{\partial^2 \phi}{\partial k_{hy}^2} &= -\frac{dz}{4\omega} \left\{ \frac{\left(\frac{1}{v(\mathbf{r},z)^2} - p_{rx}^2\right)}{\left(\frac{1}{v(\mathbf{r},z)^2} - \left(p_{rx}^2 + p_{ry}^2\right)\right)^{\frac{3}{2}}} + \frac{\left(\frac{1}{v(\mathbf{s},z)^2} - p_{sx}^2\right)}{\left(\frac{1}{v(\mathbf{s},z)^2} - \left(p_{sx}^2 + p_{sy}^2\right)\right)^{\frac{3}{2}}} \right\} \leq 0
\end{aligned}$$

We derive our conclusions concerning the validity of the stationary-phase approximation from this final formula. It also highlights intrinsic limitations of the algorithm with steep dips and evanescent waves.